Backstepping High-Order Differential Neural Network Control of Flexible-Joint Manipulator

Withit Chatlatanagulchai and Peter H. Meckl, *Member, IEEE*

Abstract—We present an output-feedback control design of a two-link, flexible-joint manipulator. The control system is a combination of the Luenberger-type observer, backstepping control, variable structure control, and high-order differential neural network. Using the neural network as model identifier, we can control this complicated system without using its closed-form mathematical model. The observer provides us with the ability to design the control system from the output signals. The variable structure controller handles uncertainties arising from model identification and state estimation. Backstepping structure provides a way of applying the robust control to each subsystem. Simulation of the two-link flexible-joint manipulator is included.

I. INTRODUCTION

JOINT flexibility exists in industrial robot manipulators. It arises from driving components such as actuators, gear teeth, transmission belts, or transducers inserted in joints to measure joint torque. In some applications, flexible joints are incorporated into the design intentionally to absorb impact force and to reduce damage to the parts from accidental collision. Furthermore, joint resonant frequencies, which are located within the control bandwidth, can be excited and cause severe oscillations. The experiment in [1] suggested that joint flexibility should be taken into account in both modeling and control design if high performance is required.

However, including joint flexibility in the model brings about two main difficulties. First, the model becomes much more complicated than the rigid-joint manipulator. Second, the system is under-actuated, that is, the number of control inputs is less than the degrees of freedom, which prohibits each link from being directly actuated by the control input. This also implies that the matching property between uncertainties and control inputs is lost. Several design approaches have been proposed to successfully control the flexible-joint manipulators. A good comparison among various backstepping and passivity-based controllers is given in [2]. Control design based on singular perturbation technique can be found in [3]-[5]. Recently, some intelligent systems have been used as model identifier. This has circumvented the complexity of modeling the flexible-joint manipulator from its governing physical laws and the

identified model is in the form that is suitable for the proposed control design scheme. References [6]-[8] presented control systems of this type.

In this paper, a control system is presented for trajectory tracking of a two-link flexible-joint manipulator in a horizontal plane. A high-order differential neural network (HODNN) is used as model identifier. Differential neural network contains feedback loops and each neuron has its own state variable. High-order interaction between neurons has been shown in the literature (e.g., [9]) to have superior storage capacity to the first-order network. This type of neural network has been used mainly in dynamic system identification. In [10], HODNN is used to estimate the states of systems in the form $\dot{x} = f(x, u)$.

In the case where angular velocities are not available, an observer, based on the Luenberger-type nonlinear observer given in [11], is applied. Controller design is based on Backstepping and Lyapunov's second method. Variable structure controller is used to provide robustness to the system. Together we obtain a control system that can be designed from the measurements of link angular positions.

We have simulated a practical situation where backlash and deadzone exist at each actuator. The robot is assumed to carry a variable payload, which changes its value every five seconds. There also exist bounded additive disturbances at each subsystem. The model used in the simulation to represent the actual plant is obtained from real experimental data.

The paper is organized as follows. Section II presents the dynamic model of the two-link flexible-joint manipulator as well as models of deadzone and backlash. Section III contains details of the HODNN identifier, observer design and controller design. Simulation results are given in Section IV and our conclusion is given in Section V.

II. DYNAMICS OF TWO-LINK FLEXIBLE-JOINT MANIPULATOR

A. Dynamic Model

Consider the manipulator in Fig. 1. We use the Euler-Lagrange method, together with the following Assumption:

Assumption 1: The rotational kinetic energy of the second motor and the second sprocket is mainly due to their own rotations by neglecting the kinetic energy from the rotation of the first link.

Let $x_1 = [\theta_1, \theta_2]^T$, $x_2 = [\dot{\theta}_1, \dot{\theta}_2]^T$, $x_3 = [\theta_5, \theta_6]^T$, $x_4 = [\dot{\theta}_5, \dot{\theta}_6]^T$, and $T = [T_1, T_2]^T$ be the four state subvectors and input torque vector respectively. The state-

space model is given by

$$\dot{x}_1 = x_2 + d_{a1}(\overline{x}_4),$$
$$\dot{x}_2 = f_2(\overline{x}_4) + g_2(\overline{x}_4)(x_3 + d_{a2}(\overline{x}_4)),$$
$$\dot{x}_3 = x_4 + d_{a3}(\overline{x}_4), \qquad (1)$$
$$\dot{x}_4 = f_4(\overline{x}_4) + g_4(\overline{x}_4)(T + d_{a4}(\overline{x}_4)),$$
$$y = x_1.$$

where

$$f_2 = -M^{-1}\left[Vx_2 + F_1 + B_1(x_2 - x_4) + K_1(x_1)\right],$$
$$g_2 = M^{-1}K_1,$$
$$f_4 = -J^{-1}\left[F_2 - B_2(x_2 - x_4) - K_2(x_1 - x_3)\right], \quad g_4 = J^{-1}.$$

d_{ai} is additive disturbance that may arise from measurement noise or simply the unmodeled dynamics, e.g. friction in microscopic level.

The inertia matrix is

$$M(x_1) = \begin{bmatrix} M_{11} & M_{12} \\ M_{21} & M_{22} \end{bmatrix},$$

where

$$M_{11} = m_1 a_1^2 + m_2(l_1^2 + a_2^2) + m_4 b_1^2 + m_6 l_1^2 + J_1 + J_2$$
$$+ m_p(l_1^2 + l_2^2) + J_p + 2l_1(m_2 a_2 + m_p l_2)\cos(\theta_2),$$
$$M_{12} = M_{21} = m_2 a_2^2 + J_2 + m_p l_2^2 + J_p$$
$$+ l_1(m_2 a_2 + m_p l_2)\cos(\theta_2),$$
$$M_{22} = m_2 a_2^2 + J_2 + m_p l_2^2 + J_p.$$

$V(x_1, x_2)x_2$ represents coriolis and centrifugal functions, where V is given by

$$V(x_1, x_2) = \begin{bmatrix} 0 & -l_1(m_2 a_2 + m_p l_2) \\ & (2\dot{\theta}_1 + \dot{\theta}_2)\sin(\theta_2) \\ l_1(m_2 a_2 + m_p l_2) & 0 \\ \dot{\theta}_1 \sin(\theta_2) & \end{bmatrix}.$$

K_1, K_2 are joint flexibility matrices

$$K_1 = \begin{bmatrix} k_5 & 0 \\ 0 & k_6 \end{bmatrix}, \quad K_2 = \begin{bmatrix} k_5/r & 0 \\ 0 & k_6/r \end{bmatrix}.$$

$F_1(x_2), F_2(x_4)$ are viscous friction vectors

$$F_1(x_2) = \left[c_1\dot{\theta}_1, c_2\dot{\theta}_2\right]^T, \quad F_2(x_4) = \left[rc_3\dot{\theta}_5, rc_4\dot{\theta}_6\right]^T.$$

J represents the inertia of motors and sprockets

$$J = \begin{bmatrix} r(J_3 + J_5/r^2) & 0 \\ 0 & r(J_4 + J_6/r^2) \end{bmatrix}.$$

B_1, B_2 contain internal damping of the torsional springs

$$B_1 = \begin{bmatrix} c_5 & 0 \\ 0 & c_6 \end{bmatrix}, \quad B_2 = \begin{bmatrix} c_5/r & 0 \\ 0 & c_6/r \end{bmatrix}.$$

B. Actuator Nonlinearities

Deadzone is a static nonlinearity that describes insensitivity of the system to a small input signal. Deadzone at the input to an actuator system, e.g. DC motor, is usually caused by friction and mechanical wear. Mathematical model of deadzone is given in [12] as follows:

$$\tau = \begin{cases} m^-(u - d^-), & u \le d^-, \\ 0, & d^- < u < d^+, \\ m^+(u - d^+), & u \ge d^+, \end{cases} \qquad (2)$$

where τ is output of deadzone model, u is input to the model, m^-, m^+, d^+ are positive numbers, and d^- is a negative number.

Backlash is the difference between tooth space and tooth width of mechanical gearing system. Backlash results in a delay in the system motion. When the driving gear changes its position, the driven gear follows only after some delay. A backlash model as in [13] is given by

$$\dot{T} = \begin{cases} m\dot{\tau}, & \text{if } \dot{\tau} > 0 \text{ and } T = m(\tau - d^+) \text{ or} \\ & \text{if } \dot{\tau} < 0 \text{ and } T = m(\tau - d^-), \qquad (3) \\ 0, & \text{otherwise}, \end{cases}$$

where T is output of backlash model, τ is input to the model, m, d^+ are positive numbers and d^- is a negative number.

Fig. 2 depicts the overall plant model, where u is the designed control input, τ is output of the deadzone model, and T is the output of the backlash model, which is the input torque to actually drive the manipulator. Both τ and T usually cannot be measured directly. Note that, even though deadzone and backlash change the magnitude of the designed control input u, the difference $\|u - T\|$ is bounded.

III. CONTROL SYSTEM DESIGN

A. Identifier Design

The HODNN, used to identify the manipulator system, has four neurons. Each neuron represents each subsystem. The neural network has the following structure

$$\dot{\xi}_1 = \hat{f}_1(\overline{\xi}_4) + \hat{g}_1(\overline{\xi}_4)(\xi_2),$$
$$\dot{\xi}_2 = \hat{f}_2(\overline{\xi}_4) + \hat{g}_2(\overline{\xi}_4)(\xi_3),$$
$$\dot{\xi}_3 = \hat{f}_3(\overline{\xi}_4) + \hat{g}_3(\overline{\xi}_4)(\xi_4), \qquad (4)$$
$$\dot{\xi}_4 = \hat{f}_4(\overline{\xi}_4) + \hat{g}_4(\overline{\xi}_4)(u),$$
$$\zeta = \xi_1,$$

where $\xi_i \in \mathbb{R}^2 = [\xi_{i1}, \xi_{i2}]^T$ is the identifier state subvector. $\overline{\xi}_4$ denotes $\{\xi_1, \ldots, \xi_4\}$. $\zeta \in \mathbb{R}^2 = [\zeta_1, \zeta_2]^T$ is the output of the identifier system. $\hat{f}_i$ and $\hat{g}_i$ are vector and matrix of identified functions respectively and are given by

$$\hat{f}_i(\bullet) \in \mathbb{R}^2 = \left[\hat{f}_{i1}, \hat{f}_{i2}\right]^T, \quad \hat{g}_i(\bullet) \in \mathbb{R}^{2\times2} = \begin{bmatrix} \hat{g}_{i11} & \hat{g}_{i12} \\ \hat{g}_{i21} & \hat{g}_{i22} \end{bmatrix}.$$

Each $\hat{f}_{io}, \forall i = 1, \ldots, 4, \forall o = 1, 2$ has the following structure, (for convenience the general indexes j and k are put in parentheses)

$$\hat{f}_{io} = -a_{io}\xi_{io} + b_{hio}\left[\sum_{k=1}^{l_{hio}} w_{(k)hio}\left(\prod_{j \in I_{(k)hio}} z_j^{d_{(jk)hio}}\right)\right].$$

Each $\hat{g}_{iop}, \forall i = 1, \ldots, 4, \forall o = 1, 2, \forall p = 1, 2$ has the following structure

$$\hat{g}_{iop} = b_{giop} \left[\sum_{k=1}^{l_{giop}} w_{(k)giop} \left(\prod_{j \in I_{(k)giop}} z_j^{d_{(jk)giop}} \right) \right].$$

$a_{io}, b_{hio}, b_{giop}$ are constant scalars. $w_{(k)hio}, w_{(k)giop}$ are neural network weights. z_j is input to the network and is defined as

$$\{z_1, z_2, z_3, \ldots, z_8\} = \{s(\xi_{11}), s(\xi_{12}), s(\xi_{21}), s(\xi_{22}), \ldots, s(\xi_{42})\},$$

where $s(\bullet)$ is logistic function of the form

$$s(\xi_{ij}) = 1/(1 + e^{-\xi_{ij}}).$$

$I_{(k)hio}$ and $I_{(k)giop}$ are not-ordered subsets of $\{1, 2, \ldots, 8\}$. $d_{(jk)hio}$ and $d_{(jk)giop}$ are non-negative integers which determine the order of interactions between inputs.

Let $\theta_{hio} = b_{hio} \left[w_{(1)hio}, w_{(2)hio}, \ldots, w_{(l_{hio})hio} \right]$ and $\theta_{giop} = b_{giop} \left[w_{(1)giop}, w_{(2)giop}, \ldots, w_{(l_{giop})giop} \right]$ be vectors of adjustable weights and let

$$z_{hio} = \left[\prod_{j \in I_{(1)hio}} z_j^{d_{(j1)hio}}, \prod_{j \in I_{(2)hio}} z_j^{d_{(j2)hio}}, \ldots, \prod_{j \in I_{(l_{hio})hio}} z_j^{d_{(jl_{hio})hio}} \right]^T$$

and

$$z_{giop} = \left[\prod_{j \in I_{(1)giop}} z_j^{d_{(j1)giop}}, \prod_{j \in I_{(2)giop}} z_j^{d_{(j2)giop}}, \ldots, \prod_{j \in I_{(l_{giop})giop}} z_j^{d_{(jl_{giop})giop}} \right]^T.$$

The coefficients $a_{io} > 0$ are design parameters and are fixed. The identifier system (4) becomes

$$\dot{\xi}_1 = \begin{bmatrix} -a_{11}\xi_{11} + \theta_{h11}^T z_{h11} \\ -a_{12}\xi_{12} + \theta_{h12}^T z_{h12} \end{bmatrix} + \begin{bmatrix} \theta_{g111}^T z_{g111} & \theta_{g112}^T z_{g112} \\ \theta_{g121}^T z_{g121} & \theta_{g122}^T z_{g122} \end{bmatrix} \begin{bmatrix} \xi_{21} \\ \xi_{22} \end{bmatrix},$$

$$\vdots$$

$$\dot{\xi}_4 = \begin{bmatrix} -a_{41}\xi_{41} + \theta_{h41}^T z_{h41} \\ -a_{42}\xi_{42} + \theta_{h42}^T z_{h42} \end{bmatrix} + \begin{bmatrix} \theta_{g411}^T z_{g411} & \theta_{g412}^T z_{g412} \\ \theta_{g421}^T z_{g421} & \theta_{g422}^T z_{g422} \end{bmatrix} \begin{bmatrix} u_1 \\ u_2 \end{bmatrix},$$

$$\zeta = \xi_1.$$

(5)

It can be shown that if the actual system (1) possesses continuous functions f_i and g_i, and the functions are locally Lipschitz in their arguments on some compact sets, then for any $\varepsilon > 0$ and any finite $t_1 > 0$, there exist integers l_{hio} and l_{giop}, ideal weight vectors θ_{hio}^* and θ_{giop}^*, and $\delta > 0$ such that if $\|x(t_0) - \xi(t_0)\| \le \delta$, then

$$\sup_{t_0 \le t \le t_1} \|x(t) - \xi(t)\| \le \varepsilon,$$

that is, the solution of the actual system (1) stays close to the solution of the identifier system (5) during any finite time interval.

Since ε cannot be made arbitrarily small by adjusting design parameters, the identifier states cannot be used as a good estimation of the actual states. In the next section we will design an observer to ensure that the errors between the actual states and the observer states are bounded and the error can be made arbitrarily small by adjusting design parameters.

B. Observer Design

Consider the mapping from states to output derivatives of the actual system (1),

$$[y_1, \dot{y}_1, \ddot{y}_1, \dddot{y}_1, y_2, \dot{y}_2, \ddot{y}_2, \dddot{y}_2]^T = y_e = H(\bar{x}_4, T, \dot{T})$$

$$= \left[x_{11}, \varphi_{11}(\bar{x}_4), \varphi_{12}(\bar{x}_4, T), \varphi_{13}(\bar{x}_4, T, \dot{T}), \right.$$

$$\left. x_{12}, \varphi_{21}(\bar{x}_4), \varphi_{22}(\bar{x}_4, T), \varphi_{23}(\bar{x}_4, T, \dot{T}) \right]^T.$$

Similarly, the mapping of the identifier system (5) is given by

$$[\zeta_1, \dot{\zeta}_1, \ddot{\zeta}_1, \dddot{\zeta}_1, \zeta_2, \dot{\zeta}_2, \ddot{\zeta}_2, \dddot{\zeta}_2]^T = \zeta_e = \hat{H}(\bar{\xi}_4, u, \dot{u})$$

$$= \left[\xi_{11}, \psi_{11}(\bar{\xi}_4), \psi_{12}(\bar{\xi}_4, u), \psi_{13}(\bar{\xi}_4, u, \dot{u}), \right.$$

$$\left. \xi_{12}, \psi_{21}(\bar{\xi}_4), \psi_{22}(\bar{\xi}_4, u), \psi_{23}(\bar{\xi}_4, u, \dot{u}) \right]^T.$$

Replacing the identifier states ξ_i by observer states $\hat{x}_i$, we have

$$\hat{\zeta}_e = \hat{H}(\hat{\bar{x}}_4, u, \dot{u}) = \left[\hat{x}_{11}, \psi_{11}(\hat{\bar{x}}_4), \psi_{12}(\hat{\bar{x}}_4, u), \right.$$

$$\left. \psi_{13}(\hat{\bar{x}}_4, u, \dot{u}), \dot{x}_{12}, \psi_{21}(\hat{\bar{x}}_4), \psi_{22}(\hat{\bar{x}}_4, u), \psi_{23}(\hat{\bar{x}}_4, u, \dot{u}) \right]^T.$$

(6)

Assumption 2: Mappings H and $\hat{H}$ are invertible with respect to $\bar{x}_4$ and $\hat{x}_4$ and their inverses, $\bar{x}_4 = H^{-1}(y_e, T, \dot{T})$ and $\hat{\bar{x}}_4 = \hat{H}^{-1}(\hat{\zeta}_e, u, \dot{u})$, are smooth.

Using the above Assumption, it can be shown that

$$\dot{y}_e = A y_e + B \left[\alpha(y_e) + \beta_1(y_e) T + \beta_2(y_e) \dot{T} + \beta_3(y_e) \ddot{T} \right],$$

where $A = block - diag\{A_1, A_2\}$, $B = block - diag\{B_1, B_2\}$,

$$A_i = \begin{bmatrix} 0 & I \\ 0 & 0 \end{bmatrix} \in \mathbb{R}^{4 \times 4}, \quad B_i = [0, \ldots, 1]^T \in \mathbb{R}^4.$$

α and β_i are functions of y_e and are given by

$$\alpha = [\alpha_1, \alpha_2]^T \in \mathbb{R}^2, \quad \beta_i = [\beta_{i1}^T, \beta_{i2}^T]^T \in \mathbb{R}^{2 \times 2}.$$

The nonlinear observer is

$$\begin{bmatrix} \dot{\hat{x}}_1 \\ \dot{\hat{x}}_2 \\ \vdots \\ \dot{\hat{x}}_4 \end{bmatrix} = \begin{bmatrix} \hat{f}_1(\hat{\bar{x}}_4) + \hat{g}_1(\hat{\bar{x}}_4)\hat{x}_2 \\ \hat{f}_2(\hat{\bar{x}}_4) + \hat{g}_2(\hat{\bar{x}}_4)\hat{x}_3 \\ \vdots \\ \hat{f}_4(\hat{\bar{x}}_4) + \hat{g}_4(\hat{\bar{x}}_4)u \end{bmatrix} + \left[\frac{\partial \hat{H}(\hat{\bar{x}}_4)}{\partial \hat{\bar{x}}_4} \right]^{-1} \varepsilon^{-1} L \left[y - \hat{\zeta} \right],$$

$$\hat{\zeta} = \hat{x}_1,$$

(7)

where $\varepsilon_i = diag\{\eta, \eta^2, \ldots, \eta^4\}$, $0 < \eta \le 1$, $\varepsilon = block - diag\{\varepsilon_1, \varepsilon_2\}$, $[\partial \hat{H}(\hat{\bar{x}}_4)/\partial \hat{x}_4]$ is Jacobian of $\hat{H}$. $L = block - diag\{L_1, L_2\} \in \mathbb{R}^{8 \times 2}$, where $L_i = [l_1, l_2, l_3, l_4]^T$ is such that $s^4 + l_1 s^3 + l_2 s^2 + l_3 s + l_4$ is a Hurwitz polynomial.

From (6) and (7), we have

$$\dot{\hat{\zeta}}_e = A \hat{\zeta}_e + B \left[\hat{\alpha}(\hat{\zeta}_e) + \hat{\beta}_1(\hat{\zeta}_e) u + \ldots + \hat{\beta}_3(\hat{\zeta}_e) \ddot{u} \right]$$

$$+ \varepsilon^{-1} L \left[y - \hat{x}_1 \right].$$

Define the observer error $\tilde{\zeta}_e = \hat{\zeta}_e - y_e$. Let $C_i = [1, 0, 0, 0]$, $C = block - diag\{C_1, C_2\}$. The observer error dynamics are given by

$$\dot{\tilde{\zeta}}_e = (A - \varepsilon^{-1} L C) \tilde{\zeta}_e + B \left[\hat{\alpha}(\hat{\zeta}_e) + \hat{\beta}_1(\hat{\zeta}_e) u + \ldots + \hat{\beta}_3(\hat{\zeta}_e) \right.$$

$$\left. \ddot{u} \right] - B \left[\alpha(y_e) + \beta_1(y_e) T + \ldots + \beta_3(y_e) \ddot{T} \right].$$

Define another coordinate transformation $\tilde{v} = \varepsilon' \tilde{\zeta}_e$ where $\varepsilon_i' = diag\left[1/\eta^3, 1/\eta^2, 1/\eta, 1 \right]$, $\varepsilon' = block - diag\{\varepsilon_1', \varepsilon_2'\}$. Let P_i be the solution of the Lyapunov equation

$P_i(A_i - L_iC_i) + (A_i - L_iC_i)^T P_i = -I$, the derivative of a Lyapunov function $V = \tilde{v}^T P \tilde{v} > 0$ where $P = block-diag\{P_1, P_2\}$, is given by

$$\dot{V} = -\tilde{v}^T \tilde{v}/\eta + 2\tilde{v}^T PB\left[\hat{\alpha}\left(\hat{\zeta}_e\right) + \hat{\beta}_1\left(\hat{\zeta}_e\right)u + \ldots + \hat{\beta}_3\left(\hat{\zeta}_e\right)\right.$$
$$\left. \ddot{u}\right] - 2\tilde{v}^T PB\left[\alpha\left(y_e\right) + \beta_1\left(y_e\right)T + \ldots + \beta_3\left(y_e\right)\ddot{T}\right].$$

From the facts that

$$\left|\hat{\alpha}\left(\hat{\zeta}_e\right) - \alpha\left(\hat{\zeta}_e\right)\right| \le k_1, \left|\hat{\beta}_i\left(\hat{\zeta}_e\right) - \beta_i\left(\hat{\zeta}_e\right)\right| \le k_{2,i}, \ i=1,\ldots,3,$$

where $k_1, k_{2,i}$ are bounded constants, $\alpha(\bullet), \beta_i(\bullet)$ are Lipschitz, input u and hence T are bounded, and $\|u - T\|$ is bounded, we have

$$\left| \begin{array}{l} \hat{\alpha}\left(\hat{\zeta}_e\right) + \hat{\beta}_1\left(\hat{\zeta}_e\right)u + \ldots + \hat{\beta}_3\left(\hat{\zeta}_e\right)\ddot{u} - \alpha\left(y_e\right) \\ -\beta_1\left(y_e\right)T - \ldots - \beta_3\left(y_e\right)\ddot{T} \end{array} \right| \le k_3 + k_4\left|\tilde{\zeta}_e\right|,$$

where k_3, k_4 are non-negative constants. Thus we have

$$\dot{V} \le -\|\tilde{v}\|^2/\eta + 2k_3\|P\|\|\tilde{v}\| + 2k_4\|P\|\|\tilde{v}\|^2.$$

By using part of $-\|\tilde{v}\|^2/\eta$ to dominate $2k_3\|P\|\|\tilde{v}\|$ for large $\|\tilde{v}\|$, it can be shown that $\tilde{v}$ and hence $\tilde{\zeta}_e$ are globally uniformly ultimately bounded (GUUB). From Assumption 2, $\|x - \hat{x}\|$ is GUUB.

C. Controller Design

Since actual states are not available, the objective of the controller is to reduce the error between observer state and desired state of each subsystem.

Let $e_j = \hat{x}_j - x_{jd}, j=1,\ldots,4$ be those errors. Let $\tilde{x}_j = \hat{x}_j - x_j, j=1,\ldots,4$ be the errors between observer states and actual states and $\tilde{\theta}_{(\cdot)} = \theta_{(\cdot)} - \theta_{(\cdot)}^*$ be the error between the weight used in the identifier system and the ideal weight.

From universal approximator property of the HODNN, we have $\left|h_{1o} - \theta_{h1o}^{*T}z_{h1o}\right| \le \varepsilon_{h1o}$, $\left|g_{1op} - \theta_{g1op}^{*T}z_{g1op}\right| \le \varepsilon_{g1op}$, $\forall o = 1,2, \forall p = 1,2$. From the result in identifier design section, we have $\left|\xi_{1o} - x_{1o}\right| \le \varepsilon_{1o}, \forall o = 1,2$. From the smoothness of f_j, g_j in (1) and $\hat{f}_j, \hat{g}_j$ in (7), we have $\left|\dot{\tilde{x}}_{1o}\right| \le \varepsilon_{\dot{x}1o}, \forall o = 1,2$. This leads to the following inequality

$$K_{1o}^{*T}\varphi_{1o} \ge \left|h_{1o} - \theta_{h1o}^{*T}z_{h1o}\right| + \left|a_1\left(\xi_{1o} - x_{1o}\right)\right| + \left|\dot{\tilde{x}}_{1o}\right|$$
$$+ \left|\left(g_{1o1} - \theta_{g1o1}^{*T}z_{g1o1}\right)x_{21d}\right| + \left|\left(g_{1o2} - \theta_{g1o2}^{*T}z_{g1o2}\right)x_{22d}\right|,$$

where

$$K_{1o}^{*} = \left[\varepsilon_{h1o}, \varepsilon_{1o}, \varepsilon_{\dot{x}1o}, \varepsilon_{g1o1}, \varepsilon_{g1o2}\right]^T,$$
$$\varphi_{1o} = \left[1, |a_1|, 1, |x_{21d}|, |x_{22d}|\right]^T, \forall o = 1,2.$$

Let the virtual control of the first subsystem be

$$x_{2d} = \left[x_{21d}, x_{22d}\right]^T$$
$$= -\begin{bmatrix} \hat{g}_{111} & \hat{g}_{112} \\ \hat{g}_{121} & \hat{g}_{122} \end{bmatrix}^{-1}\left(c_1 e_1 + \begin{bmatrix} \hat{f}_{11} \\ \hat{f}_{12} \end{bmatrix} - \begin{bmatrix} \dot{x}_{11d} \\ \dot{x}_{12d} \end{bmatrix} + \begin{bmatrix} u_{2dvsc1} \\ u_{2dvsc2} \end{bmatrix}\right),$$

where the smooth variable structure control is given by

$$u_{2dvsco} = K_{1o}^T\overline{\varphi}_{1o}, \forall o = 1,2,$$

where

$$\overline{\varphi}_{1o} = \left[\frac{2}{\pi}\arctan\left(\frac{e_{1o}}{\mu_1}\right), |a_1|\frac{2}{\pi}\arctan\left(\frac{e_{1o}}{\mu_1}|a_1|\right), \frac{2}{\pi}\arctan\left(\frac{e_{1o}}{\mu_1}\right)\right.$$
$$\left., |x_{21d}|\frac{2}{\pi}\arctan\left(\frac{e_{1o}}{\mu_1}|x_{21d}|\right), |x_{22d}|\frac{2}{\pi}\arctan\left(\frac{e_{1o}}{\mu_1}|x_{22d}|\right)\right]^T,$$

$\forall o = 1,2$. μ_1 is a small positive number. K_{1o} approximates K_{1o}^*. The $\dot{e}_1$ equation becomes

$$\dot{e}_1 = \dot{\hat{x}}_1 - \dot{x}_{1d} = \begin{bmatrix} h_{11} - \theta_{h11}^{*T}z_{h11} \\ h_{12} - \theta_{h12}^{*T}z_{h12} \end{bmatrix} + a_1\begin{bmatrix} \xi_{11} - x_{11} \\ \xi_{12} - x_{12} \end{bmatrix} + \begin{bmatrix} \dot{\tilde{x}}_{11} \\ \dot{\tilde{x}}_{12} \end{bmatrix}$$
$$+ g_1 e_2 - c_1 e_1 + \begin{bmatrix} g_{111} - \theta_{g111}^{*T}z_{g111} & g_{112} - \theta_{g112}^{*T}z_{g112} \\ g_{121} - \theta_{g121}^{*T}z_{g121} & g_{122} - \theta_{g122}^{*T}z_{g122} \end{bmatrix}\begin{bmatrix} x_{21d} \\ x_{22d} \end{bmatrix}$$
$$- \begin{bmatrix} \tilde{\theta}_{h11}^T z_{h11} \\ \tilde{\theta}_{h12}^T z_{h12} \end{bmatrix} - \begin{bmatrix} \theta_{g111}^{*T}z_{g111} & \theta_{g112}^{*T}z_{g112} \\ \theta_{g121}^{*T}z_{g121} & \theta_{g122}^{*T}z_{g122} \end{bmatrix}\begin{bmatrix} x_{21d} \\ x_{22d} \end{bmatrix} - \begin{bmatrix} K_{11}^T\overline{\varphi}_{11} \\ K_{12}^T\overline{\varphi}_{12} \end{bmatrix}.$$

Similarly, the virtual control of the ith subsystem, $2 \le i \le 3$, is given by

$$x_{(i+1)d} = \begin{bmatrix} x_{(i+1)1d} \\ x_{(i+1)2d} \end{bmatrix} = -\begin{bmatrix} \hat{g}_{i11} & \hat{g}_{i12} \\ \hat{g}_{i21} & \hat{g}_{i22} \end{bmatrix}^{-1}\left(\begin{bmatrix} g_{(i-1)11U} & g_{(i-1)12U} \\ g_{(i-1)21U} & g_{(i-1)22U} \end{bmatrix}e_{i-1}\right.$$
$$\left. + c_i e_i + \left[\hat{f}_{i1}, \hat{f}_{i2}\right]^T - \left[\dot{x}_{i1d}, \dot{x}_{i2d}\right]^T + \left[u_{(i+1)dvsc1}, u_{(i+1)dvsc2}\right]^T\right).$$

where $\left|g_{iop}\right| \le g_{iopU}, \forall i = 1,\ldots,4, \forall o = 1,2, \forall p = 1,2$. The variable structure control $u_{(i+1)dvsco}, \forall o = 1,2$ is similar to the previous subsystem. The $\dot{e}_i$ equation can be found similarly.

The actual control input is given by

$$u = \begin{bmatrix} u_1 \\ u_2 \end{bmatrix} = -\begin{bmatrix} \hat{g}_{411} & \hat{g}_{412} \\ \hat{g}_{421} & \hat{g}_{422} \end{bmatrix}^{-1}\left(\begin{bmatrix} g_{311U} & g_{312U} \\ g_{321U} & g_{322U} \end{bmatrix}e_3 + c_4 e_4\right.$$
$$\left. + \begin{bmatrix} \hat{f}_{41} \\ \hat{f}_{42} \end{bmatrix} - \begin{bmatrix} \dot{x}_{41d} \\ \dot{x}_{42d} \end{bmatrix} + \begin{bmatrix} u_{5dvsc1} \\ u_{5dvsc2} \end{bmatrix}\right). \quad (8)$$

The $\dot{e}_4$ equation can be found similarly. Choose the Lyapunov function of the whole system as

$$V = \sum_{i=1}^{4}\left\{\frac{1}{2}e_i^T e_i + \sum_{o=1}^{2}\sum_{p=1}^{2}\left\{\frac{1}{2}\tilde{\theta}_{giop}^T\Gamma_{giop}^{-1}\tilde{\theta}_{giop}\right\}\right.$$
$$\left. + \sum_{o=1}^{2}\left\{\frac{1}{2}\tilde{\theta}_{hio}^T\Gamma_{hio}^{-1}\tilde{\theta}_{hio} + \frac{1}{2}\tilde{K}_{io}^T\Gamma_{kio}^{-1}\tilde{K}_{io}\right\}\right\},$$

where $\tilde{K}_{io} = K_{io} - K_{io}^*, \forall o = 1,2$, and $\Gamma_{giop}, \Gamma_{hio}, \Gamma_{kio}$ are positive constants. Let the weight adaptation laws be

$$\dot{K}_{io} = \dot{\tilde{K}}_{io} = \Gamma_{kio}\left[\overline{\varphi}_{io}e_{io} - \sigma_{kio}K_{io}\right],$$
$$\dot{\theta}_{hio} = \dot{\tilde{\theta}}_{hio} = \Gamma_{hio}\left[z_{hio}e_{io} - \sigma_{hio}\theta_{hio}\right],$$
$$\dot{\theta}_{giop} = \dot{\tilde{\theta}}_{giop} = \Gamma_{giop}\left[z_{giop}e_{io}x_{(i+1)dp} - \sigma_{giop}\theta_{giop}\right], \quad (9)$$
$$\forall i = 1,\ldots,4, \forall o = 1,2, \forall p = 1,2.$$

For $i = 4$, replace $x_{(i+1)dp}$ by u_p. $\sigma_{kio}, \sigma_{hio}, \sigma_{giop}$ are positive constants. Using the following facts

$$0 \leq |\alpha| - \alpha (2/\pi) \arctan (\alpha/\mu) \leq 0.2785\mu, \quad \forall \alpha \in \mathbb{R},$$

$$2\tilde{K}_{io}^T K_{io} = \left\| \tilde{K}_{io} \right\|^2 + \left\| K_{io} \right\|^2 - \left\| K_{io}^* \right\|^2 \geq \left\| \tilde{K}_{io} \right\|^2 - \left\| K_{io}^* \right\|^2,$$

$$2\tilde{\theta}_{hio}^T \theta_{hio} = \left\| \tilde{\theta}_{hio} \right\|^2 + \left\| \theta_{hio} \right\|^2 - \left\| \theta_{hio}^* \right\|^2 \geq \left\| \tilde{\theta}_{hio} \right\|^2 - \left\| \theta_{hio}^* \right\|^2,$$

$$2\tilde{\theta}_{giop}^T \theta_{giop} = \left\| \tilde{\theta}_{giop} \right\|^2 + \left\| \theta_{giop} \right\|^2 - \left\| \theta_{giop}^* \right\|^2 \geq \left\| \tilde{\theta}_{giop} \right\|^2 - \left\| \theta_{giop}^* \right\|^2,$$

the derivative $\dot{V}$ is given by

$$\dot{V} \leq \sum_{i=1}^{4} \left\{ -e_i^T c_i e_i - \sum_{o=1}^{2}\sum_{p=1}^{2} \left\{ \frac{\sigma_{giop}}{2} \left\| \tilde{\theta}_{giop} \right\|^2 \right\} \right.$$
$$\left. -\sum_{o=1}^{2} \left\{ \frac{\sigma_{kio}}{2} \left\| \tilde{K}_{io} \right\|^2 + \frac{\sigma_{hio}}{2} \left\| \tilde{\theta}_{hio} \right\|^2 \right\} + \phi_i \right\},$$

where

$$\phi_i = \sum_{o=1}^{2} \left\{ 0.2785\mu_i \left(\varepsilon_{hio} + \varepsilon_{io} + \varepsilon_{\dot{x}io} + \varepsilon_{gio1} + \varepsilon_{gio2} \right) \right\}$$
$$+ \sum_{o=1}^{2}\sum_{p=1}^{2} \left\{ \frac{\sigma_{giop}}{2} \left\| \tilde{\theta}_{giop}^* \right\|^2 \right\} + \sum_{o=1}^{2} \left\{ \frac{\sigma_{kio}}{2} \left\| \tilde{K}_{io}^* \right\|^2 + \frac{\sigma_{hio}}{2} \left\| \tilde{\theta}_{hio}^* \right\|^2 \right\}.$$

Let $\varsigma = \min_{1 \leq i \leq 4} \{2c_i\} \geq 0$, $\delta = \sum_{i=1}^{4} \phi_i \geq 0$ and choose

$$\sigma_{hio} \geq \varsigma \lambda_{\max} \left\{ \Gamma_{hio}^{-1} \right\}, \sigma_{giop} \geq \varsigma \lambda_{\max} \left\{ \Gamma_{giop}^{-1} \right\},$$

$$\sigma_{kio} \geq \varsigma \lambda_{\max} \left\{ \Gamma_{kio}^{-1} \right\}, \quad i = 1,\ldots,4,$$

we have $\dot{V} \leq -\varsigma V + \delta$. From this point on, it can be shown using standard nonlinear analysis that the error trajectories $e_i, \tilde{K}_{io}, \tilde{\theta}_{giop}, \tilde{\theta}_{hio}$ are GUUB.

IV. SIMULATION RESULT

The dynamic system used to represent an actual plant in our simulation is obtained from actual experiment. From standard least-square technique, we obtain the plant (1) as follows:

$$M(x_1) = \begin{bmatrix} 0.201 + 0.06\cos\theta_2 & 0.0266 + 0.03\cos\theta_2 \\ 0.0266 + 0.03\cos\theta_2 & 0.0266 \end{bmatrix},$$

$$V(x_1, x_2) = \begin{bmatrix} 0 & -0.03(2\dot{\theta}_1 + \dot{\theta}_2)\sin\theta_2 \\ 0.03\dot{\theta}_1 \sin\theta_2 & 0 \end{bmatrix},$$

$$K_1 = 0.4I^{2\times 2}, K_2 = 0.075I^{2\times 2}, J = \begin{bmatrix} 0.017 & 0 \\ 0 & 0.014 \end{bmatrix},$$

$$B_1 = \begin{bmatrix} 0.016 & 0 \\ 0 & 0.016 \end{bmatrix}, B_2 = \begin{bmatrix} 0.003 & 0 \\ 0 & 0.003 \end{bmatrix},$$

$$F_1(x_2) = \begin{bmatrix} 0.02\dot{\theta}_1 \\ 0.02\dot{\theta}_2 \end{bmatrix}, F_2(x_4) = \begin{bmatrix} 0.056\dot{\theta}_5 \\ 0.056\dot{\theta}_6 \end{bmatrix}.$$

We simulate deadzone and backlash by using the following parameters. For deadzone model (2), we have $d^- = -0.1, d^+ = 0.1, m^- = m^+ = 1$. For backlash model (3), we use $d^- = -0.1, d^+ = 0.1, m = 1$. External disturbances are as follows: $d_{a1} = d_{a4} = [0.01\sin(\theta_1\dot{\theta}_1), \arctan(\theta_1\dot{\theta}_2)]^T$, $d_{a2} = d_{a3} = [0.001 \, \text{randn}(2,1)]^T$, where *randn* represents white noise.

To simulate payload changes, we multiply $M(x_1)$ and $V(x_1, x_2)$ matrices by three from 5 to 9 seconds, 15 to 19

seconds, 25 to 29 seconds, and 35 to 39 seconds.

The identifier system (5) has the following parameters $a_{io} = 15, \forall i = 1,\ldots,4, \forall o = 1,2$. The inputs to the network are given by $z_{h21} = z_{h22} = [z_1, z_2, z_3, z_4, z_3 z_4, z_3^2, z_4^2, z_7, z_8]$, $z_{h41} = [z_1, z_3, z_5, z_7]$, $z_{h42} = [z_2, z_4, z_6, z_8]$, $z_{g211} = z_{g212} = z_{g221} = z_{g222} = z_2$. All other z_{hio} and z_{giop} are set to one.

The observer (7) has the following parameters $l_1 = 113, l_2 = 3332, l_3 = 9220, l_4 = 6000, \eta = 0.1$.

The controller (8) has the following parameters $g_{111U} = g_{122U} = g_{311U} = g_{322U} = 1, g_{212U} = g_{221U} = 8,$

$g_{112U} = g_{121U} = g_{312U} = g_{321U} = 0, g_{211U} = 4, g_{222U} = 30,$

$c_i = 50, \mu_i = 0.1, \forall i = 1,\ldots,4.$

Input saturation limits are set at ± 15.

The weight update law (9) has the following parameters $\Gamma_{kio} = 10, \sigma_{kio} = 1, \Gamma_{hio} = 10, \sigma_{hio} = 1,$

$\Gamma_{giop} = 0.01, \sigma_{giop} = 0, \forall i = 1,\ldots,4, \forall o = 1,2, \forall p = 1,2.$

All initial values are set at zeros except the following $\theta_{g211}(0) = 6, \theta_{g212}(0) = -5, \theta_{g221}(0) = 2, \theta_{g222}(0) = 20,$

$\theta_{g411}(0) = 60, \theta_{g412}(0) = 0, \theta_{g421}(0) = 0, \theta_{g422}(0) = 70,$

$\theta_{f41}(0) = \theta_{f42}(0) = 0.5.$

Sampling period is 1 ms. The desired trajectory is obtained from passing a square wave of amplitude 10, with zero mean, and 20-second period into the filter $1/(s+2)^3$. Simulation result is given in Fig. 3. The control system achieves good overall tracking performance as can be seen from the result in Fig. 3(a-d). Fig. 3(e-f) show some of the actual functions versus their estimated values. Control inputs u_1 and u_2, are given in Fig. 3(g-h). In Fig. 3(i-l), scatter plots show the effect of deadzone and backlash on the magnitude of the desired control input.

V. CONCLUSION

The contribution of this paper is that it presents a way of controlling the manipulator when joint flexibility is directly taken into account. Practical issues like deadzone, backlash, external disturbance, and payload changes are also considered. The control system presented in the paper is able to overcome the uncertainties arising from those in practice by treating them as bounded uncertainties. When observer is implemented, we are able to control the manipulator using link angular positions. The intelligent system used as model identifier can adjust itself when there are changes in the system. The adjustment is in the direction of reduction of the tracking error. Robust control from a variable structure controller is inserted into each subsystem through a backstepping structure. As a result, overall good tracking performance is achieved.

REFERENCES

[1] L. M. Sweet and M. C. Good, "Re-definition of the robot motion control problem: effects of plant dynamics drive system constraints, and user requirements," *Proc. of 23rd IEEE Conf. on Decision and Control*, Las Vegas, NV, 1984, pp. 724-731.

[2] B. Brogliato, R. Ortega and R. Lozano, "Global tracking controllers for flexible-joint manipulators: a comparative study," *Automatica*, vol. 31, no. 7, pp. 941-956, July 1995.

[3] S. S. Ge, "Adaptive controller design for flexible joint manipulators," *Automatica,* vol. 32, no. 2, pp. 273-278, Feb. 1996.

[4] J. Hernandez and J. P. Barbot, "Sliding observer-based feedback control for flexible joints manipulator," *Automatica*, vol. 32, no. 9, pp. 1243-1254, Sep. 1996.

[5] F. Ghorbel, J. Y. Hung, and M. W. Spong, "Adaptive control of flexible-joint manipulators," *Control Systems Magazine,* vol. 9, no. 7, pp. 9-13, Dec. 1989.

[6] C. W. Park and Y. W. Cho, "Adaptive tracking control of flexible joint manipulator based on fuzzy model reference approach," in *IEE Proc. Control Theory and Applications*, 2003, pp. 198-204.

[7] L. C. Lin and T. E. Lee, "Integrated PID-type learning and fuzzy control for flexible-joint manipulators," *Journal of Intelligent and Robotic Systems*, vol. 18, no. 1, pp. 47-66, Jan. 1997.

[8] S. B. Lee and H. S. Cho, "Neural network-based control of balanced robotic manipulators with joint flexibility," *Mechatronics*, vol. 1, no. 4, pp. 487-507, 1991.

[9] P. Paretto and J. J. Niez, "Long term memory storage capacity of multiconnected neural networks," *Biol. Cybern.,* vol. 54, pp. 53-63, 1986.

[10] E. B. Kosmatopoulos, M. M. Polycarpou, M. A. Christodoulou, and P. A. Ioannou, "High-order neural network structures for identification of dynamical systems," *IEEE Trans. Neural Networks*, vol. 6, no. 2, pp. 422-430, March 1995.

[11] J. T. Spooner, M. Maggiore, R. Ordonez and K. M. Passino, *Stable Adaptive Control and Estimation for Nonlinear Systems.* New York: Wiley Interscience, 2002.

[12] G. Tao and P. V. Kokotovic, *Adaptive Control of Systems with Actuator and Sensor Nonlinearities*. New York: Wiley, 1996.

[13] F. L. Lewis, J. Campos, and R. Selmic, *Neuro-Fuzzy Control of Industrial Systems with Actuator Nonlinearities*. Philadelphia: SIAM, 2002.
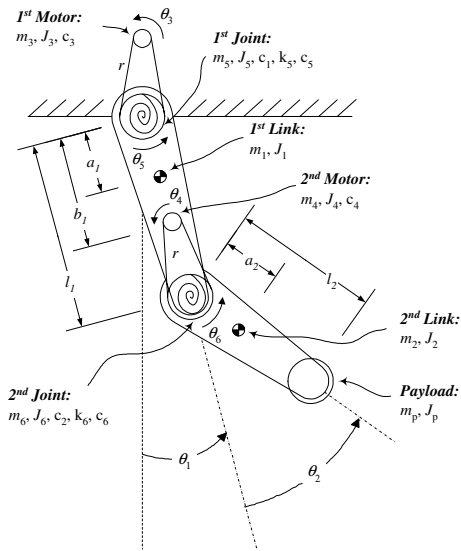
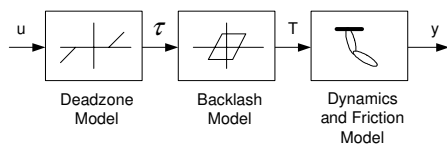Fig. 1. Schematic diagram of the two-link flexible-joint manipulator.

Fig. 2. Deadzone and backlash models are incorporated into the dynamic model of the two-link flexible-joint manipulator.
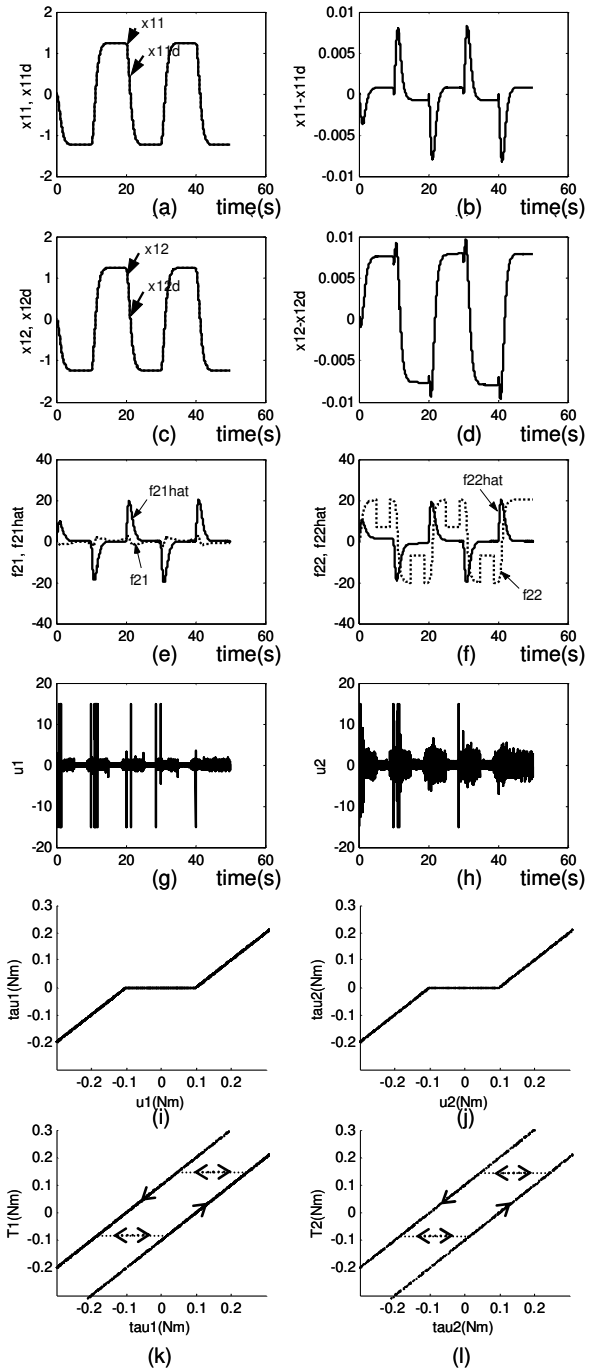

Fig. 3. (a) θ_1 versus θ_{1d}. (b) Tracking error $\theta_1 - \theta_{1d}$. (c) θ_2 versus θ_{2d}. (d) Tracking error $\theta_2 - \theta_{2d}$. (e) f_{21} versus $\hat{f}_{21}$. (f) f_{22} versus $\hat{f}_{22}$. (g) Actual input u_1. (h) Actual input u_2. (i) Plot between u_1 and τ_1. (j) Plot between u_2 and τ_2. (k) Plot between τ_1 and T_1. (l) Plot between τ_2 and T_2.